

Propulsion System Performance Enhancements on REMUS AUVs

Ben Allen

Woods Hole Oceanographic Institution
Woods Hole, MA 02543
email: ballen@whoi.edu

William S. Vorus

University of New Orleans
New Orleans, LA 70148
email: wvorus@uno.edu

Timothy Prestero

Massachusetts Institute of Technology
Cambridge, MA 02139
email: tprester@mit.edu

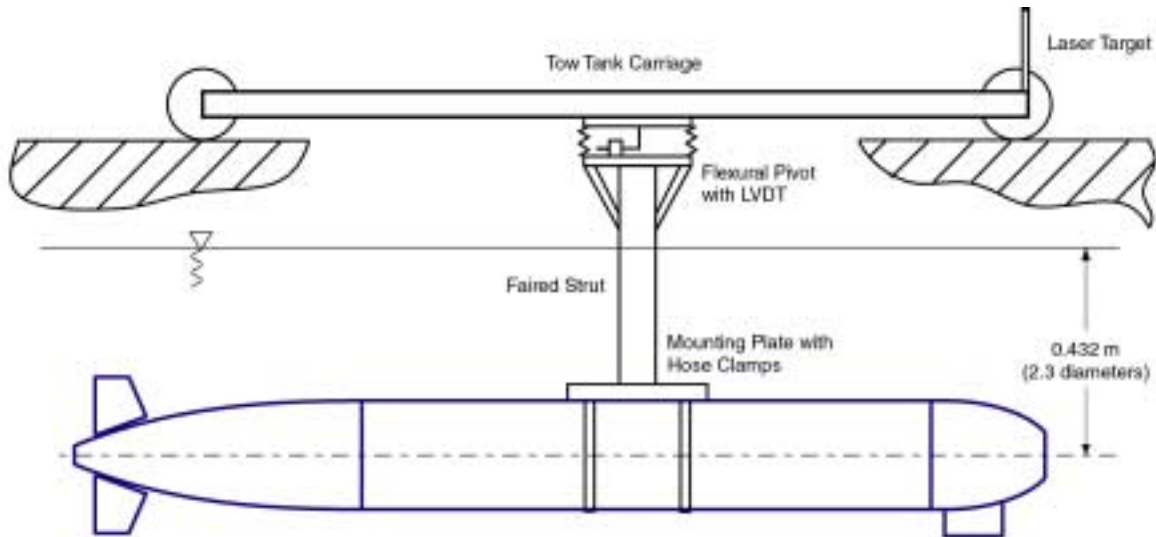


Fig. 1 Vehicle on Flexural Pivot

Abstract- This paper details recent efforts on drag reduction, vehicle shape and propulsion system modifications, and propeller design for the REMUS class of autonomous underwater vehicles (AUV).

Drag reduction was accomplished by tow-tank measurements of an existing design to itemize the sources of drag. The vehicle shape and main propulsion system were modified to use magnetic torque transfer through a seawater collar to eliminate a rotating shaft seal. Propeller design efforts consisted first of a trade-off analysis of blade number, RPM, vehicle speed and blade shape to determine an optimum design and then refinement of that design for a production version. The combined effect of these efforts resulted in a four fold reduction in propulsion power at the same speed of the previous design, and an increase in maximum achievable speed by almost a factor of two.

These propulsion system performance improvements combined with recent changes in energy capacity for the vehicle result in a total per mission range of 120 km at 1.5 m/s for an endurance of 20 hours.

This work was supported by the Office of Naval Research under contract N00014-99-1-2080 and by the Naval Sea Systems Command (NAVSEA PMS-325-J) under contract N00024-00-C-6304.

I. INTRODUCTION

One of the more important attributes of any AUV is its endurance, or the range and speed that the vehicle has available to accomplish its mission. An increase in propulsion system efficiency corresponds to a longer range for a given speed, or the ability to cover the same distance in a reduced time. Any efforts to improve the overall efficiency will result in a more useful vehicle.

REMUS is a low-cost, man-portable AUV design with approximately 1000 hours of water time over hundreds of missions on 10 vehicles [1][2]. The vehicle design has been very successful in demonstrating the usefulness of AUVs in the ocean [3], however it is limited in its range and speed [4]. The existing design system used model airplane propellers with a brushed DC motor, propeller shaft and shaft seal. A recent design effort entailed modifications to this design to provide significantly greater propulsion performance.

It is not possible to determine the difference between effects of hull drag coefficient and propeller efficiency in open water vehicle tests when neither the actual vehicle drag coefficient nor propeller efficiencies are known.

Therefore the first step in the design process entailed quantifying the sources of drag in a tow-tank on an existing vehicle, and then determining what improvements were possible.

The next phase was a two-fold re-design effort. The first effort was to reduce the drag of the vehicle by streamlining and fairing where possible based on tow-tank test results. The second step was to maximize the efficiency in delivery of power to the propeller shaft by selecting a more efficient motor (brushless DC) and eliminate as many power losses as possible (shaft seal).

The results of these re-design efforts were then used as input parameters to evaluate a series of possible propeller designs from which an optimal design was chosen. In-water tests of the new design were then used to compare with the existing design.

II. TOW-TANK MEASUREMENTS

In the spring of 1999, the authors ran a series of tow tank experiments with the REMUS vehicle. The purpose of these experiments was to measure the vehicle axial drag coefficient and the thrust of the vehicle propeller, and to assist in estimating the overall efficiency of the vehicle propulsion system. The experiments involved recording axial and lateral drag data for a range of vehicle speeds and hull configurations, as well as thrust data from the vehicle for a range of propeller speeds.

A. Experimental Set-up

The experiments were conducted at the University of Rhode Island Tow Tank, located in the Sheets Building on the Narragansett Bay Campus. The URI tow tank, which was filled with fresh water, is approximately 30 meters long by 3.5 meters wide by 1.5 meters deep (100 by 12 by 5 feet). The tow tank carriage has a useful run of almost 21 meters (70 feet). See Fig. 1 and Fig. 2 for a diagram of the tow tank layout.

Given the large size of the tank relative to the vehicle, we were able to use a full-scale REMUS vehicle during the tests, rather than a scale model. The vehicle was suspended in the water by a faired strut, which was connected to the towing carriage on the bottom plate of a flexural pivot. See Fig. 1 for a diagram of the tow-carriage setup and vehicle mounting; see Fig 3 for a picture of the same.

The motion of the plate was measured using two orthogonally-mounted linear variable differential transformers (LVDTs). The LVDT output signals were amplified and electronically filtered, then transmitted to the data station where they were plotted on a strip chart recorder and sampled by an analog-to-digital board connected to a laptop PC.



Fig. 2 Plan View of Experimental Setup

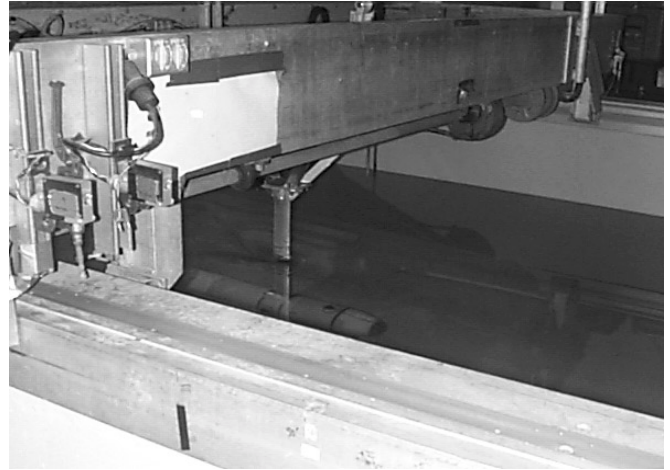


Fig. 3. REMUS vehicle mounting, showing tank carriage and strut.

The carriage speed was measured using a Nova Ranger NR-100 laser range finder. The range finder signal was sent directly to the analog-to-digital board.

For a given run, data was collected from the three channels simultaneously—vehicle axial drag, vehicle lateral drag, and carriage speed—at a frequency of 400 Hz per channel. To remove sensor noise and the high-frequency strut and carriage vibrations, the data was filtered in post-processing using a zero-phase forwards and reverse digital filter of order 250 and a cut-off frequency of 2.5 Hz.

Since the lateral flexures of the pivot assembly were quite stiff compared to the axial flexures, the lateral LVDT was used more as a rough indicator of strut, vehicle and fin alignment.

B. Drag Runs

The tow tank runs were conducted at five different speeds with a maximum of 1.5 meters per second or 3 knots, an operating speed of the vehicle. The experiments involved a variety of vehicle configurations. After spending several sessions preparing and calibrating the lab equipment, the authors ran four days of vehicle tests.

Table 1 gives the dates and details of these experimental runs. Note that in the last set of runs, the vehicle fins were removed. This was to check the repeatability of the results, as it was challenging to maintain the alignment of the fins between individual runs.

TABLE 1
REMUS DRAG RUNS

Date	Filename	Vehicle (Notes)
09 Jun 99	Remxfps7	WHOI1
16 Jun 99	Remdxfps8	WHOI1 (DOCK2 tail)
16 Jun 99	Remdxfps8b	WHOI1 (DOCK2 tail)
16 Jun 99	Rnfdxfps8	WHOI1 (DOCK2 tail, no fins)
16 Jun 99	Rnfdxfps8b	WHOI1 (DOCK2 tail, no fins)

C. Experimental Results

Fig. 4 shows a plot of forward speed versus vehicle axial drag for the different configurations. These data were averaged to find a relationship between forward velocity and axial drag, based on the following formula:

$$c_d = 2F_d / (\rho A_f v^2) \quad (1)$$

where F_d is the measured drag force (after subtraction of strut drag), ρ the fluid density (999.1 kg/m^3), A_f the vehicle frontal area (0.029 meters), v the measured vehicle forward velocity, and c_d the vehicle drag coefficient. This resulted in an experimental average drag coefficient of 0.267. The resulting parabolic fit is also plotted in Fig. 4.

Although the vehicle was towed at a depth of 2.3 body diameters, a significant amount of wave-making was noticed in the tank for carriage speeds above one meter per second. This additional wave-making drag can be seen in Fig. 4 as a deviation in the experimental data from the parabolic curve fit at higher carriage speeds.

D. Component Drag Analysis

Bottaccini [5] and Hoerner [6] suggests a drag coefficient of 0.08 to 0.1 for torpedo shapes similar to REMUS, i.e. for fineness ratios (length over maximum diameter) of 6 to 11. Given the experimentally measured drag coefficient of 0.267, it is obvious that the various hull protrusions contribute significantly to the total vehicle drag.

Table 2 lists the different vehicle components and their estimated contributions to the total vehicle drag. The drag coefficient value for the vehicle hull is from Myring [7] for a 'B' hull contour. The drag coefficient estimates for the vehicle components are taken from Hoerner [6]. All estimates assume a vehicle operating speed of 1.54 meters per second (3 knots). The resulting estimate for total drag yields, by Equation 1, an overall drag coefficient of 0.26, which compares well with the experimental results.

TABLE 2
REMUS COMPONENT-BASED DRAG ANALYSIS – STANDARD VEHICLE

ea	Cd	length m	Width m	Diam. m	Area m ²	Drag N
Myring Hull	1			0.19	2.E-04	3.39
Fins	4	0.09	0.08		5.E-05	0.62
LBL Transducer	1	0.03	0.05		1.E-05	2.07
Nose Pockets	3			0.03	4.E-06	2.68
Blunt Nose	1					0.00
SSS Transducers	2	0.04	0.04		1.E-05	1.47
ADCP Transducers	8			0.05	1.E-05	3.86
Total Vehicle Drag:						8.77
Effective Cd:						0.26

III. VEHICLE MODIFICATIONS

A. Vehicle Shape Changes

The vehicle shape was modified based on the results of the tow-tank tests. As many of the drag sources as possible were either eliminated or faired to minimize drag. Specifically, sensor pockets in the nose cap were removed, the blunt nose was extended to a full ellipse, the long baseline (LBL) transducer was cast into a foil section potting (NACA 0024) and the sidescan sonar transducers were streamlined to reduce drag. The effect of all these changes reduced the drag coefficient of the existing vehicle with sidescan sonar and ADCP from 0.42 (See Table 3) down to an estimated 0.20 (see Table 4) for the new vehicle configured with sidescan sonar and ADCP (see Fig. 5).

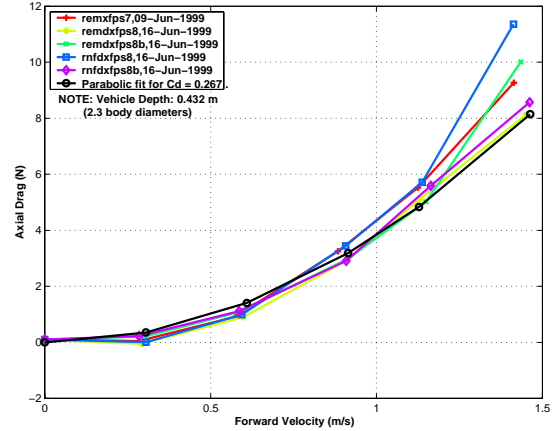


Fig. 4. Forward speed vs. vehicle axial drag.

TABLE 3
REMUS COMPONENT-BASED DRAG ANALYSIS – EXISTING SONAR VEHICLE

	Ea	Cd	length m	width m	diam. m	Area m ²	Drag N
Myring Hull	1	0.10			0.19	2.E-04	3.39
Fins	4	0.02	0.09	0.08		5.E-05	0.62
LBL Transducer	1	1.20	0.03	0.05		1.E-05	2.07
Nose Pockets	3	1.17			0.03	4.E-06	2.68
Blunt Nose	1	?					0.00
SSS Transducers	2	0.40	0.04	0.04		1.E-05	1.47
ADCP Transducers	8	0.20			0.05	1.E-05	3.86
Total Vehicle Drag:							14.09
Effective Cd:							0.42

TABLE 4
REMUS COMPONENT-BASED DRAG ANALYSIS – NEW SIDESCAN SONAR VEHICLE

	Ea	Cd	length m	width m	Diam. M	Area m ²	Drag N
Myring Hull	1	0.10			0.19	2.E-04	3.39
Fins	4	0.02	0.09	0.08		5.E-05	0.62
LBL Transducer	1	0.20	0.03	0.05		1.E-05	0.35
SSS Transducers	2	0.40	0.01	0.04		3.E-06	0.46
ADCP Transducers	4	0.20			0.05	1.E-05	1.93
Total Vehicle Drag:							6.75
Effective Cd							0.20



Fig. 5. REMUS Vehicle with Sidescan Sonar and ADCP Transducers

B. Propulsion Motor Changes

REMUS operates over a range of speeds from 2 to 5 knots. A significant source of friction at low speeds, and hence power loss, are the wear surfaces associated with a rotating shaft seal. This dynamic shaft seal is also a challenging seal to maintain and keep reliable for extended periods of time in turbid coastal waters. A primary power loss on the existing design is the brushed DC motor which operates in an air filled compartment at an estimated 65% efficiency at 80 watts. Other sources of power losses include the coupling and bearings of a conventional drive system.

Therefore, the main propulsion system was modified to use a brushless DC motor with magnetic torque transfer through a plastic collar as a mechanism to eliminate a rotating shaft seal. The new design incorporated a motor stator housing pressed into the tail cone of the vehicle, thereby providing a good heat sink for the motor. The motor rotor was cast in polyurethane and mounted in a flooded seawater cavity where the motor rotor shaft is also the propeller shaft, thereby eliminating a coupling.

The performance of the motor is dependent upon the temperature of the windings, and the ability of the vehicle and seawater to dissipate heat. These heat dissipation values have been estimated for motor performance calculations, but have yet to be measured at different temperatures of seawater.

IV. PROPELLER DESIGN

In the summer of 1999, the authors conducted a propeller design trade-off analysis for the vehicle modified by the drag studies and propulsion system re-design. The results of the trade-off analysis led to the selection of input parameters for a final design for a propeller for REMUS.

A. Trade-off Analysis

In this propeller design trade-off analysis, all the propellers were designed using lifting-line theory, reference [2]. All non-ideal (viscous) effects were incorporated as simple skin friction drag coefficients assigned to the sections of the lifting elements according to local Reynolds number. In order to avoid premature flow separation in maintaining the condition that induction losses dominate viscous momentum losses, the propeller blade sections should be well streamlined (thin) and not too heavily loaded. The criteria adopted for avoiding flow separation and thereby maintaining the integrity of the ideal flow theory design basis was:

- 1) Restrict thickness-to-chord ratios of element sections to well less than 20%, but not less than about 4%.
- 2) Restrict lift coefficients of element sections to a maximum of 0.3.

Two and three bladed propellers with three blade shapes were investigated in the design trade-off analysis. Blade shape 1 is based on NSMB B-series propeller. Blade shape 2 has a constant chord along the radius. Blade shape 3 is a modification from blade shape 1 with increased chords towards the hub and reduced chords between 0.4R and 0.8R. All three blade-shapes have the same expended area ratio A_e/A_0 . For a 3-blade propeller, the area ratio is 0.307, and A_e/A_0 becomes 0.205 for a 2-blade propeller. These blade areas were found to be the minimum compatible with the .3 upper limit on section lift coefficient.

Four diameters: 5.5, 6., 6.5, and 7 inches were evaluated at four vessel speeds: 3.5, 4., 4.5, 5. knots. With 3 blade-shapes, 4 specified design speeds and thrusts, 4 different propeller diameters, and 2 blade numbers, the trade-off analysis resulted in a total of 96 propeller designs evaluated. The restrictions were maximum power absorption of 80 watts with torque not exceeding 2.8 in-lbs, as the reaction torque limit of the vehicle. The criteria for selection was high efficiency and high speed within the design constraints.

B. Final Design

The propeller design selected from the trade-off studies was the 5.5 inch diameter 3-bladed case with blade shape #3

In this specific detailed design, the onset flow into the propeller plane, with vehicle nominal hull boundary layer effect included, was calculated first by a three-dimension panel method. The propeller was then designed using a lifting-line representation, [8], with lifting surface corrections applied. The blade radial chord distribution was modified slightly from the blade shape No. 3 used in the trade-off analysis.

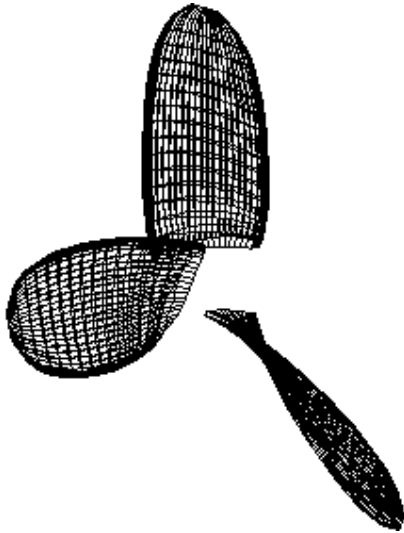
The principal characteristics of the propeller design are listed in Table 5 below and the 3-dimensional blades are shown on Figure 6.

Table 5
PROPELLER PRINCIPAL CHARACTERISTICS

Diameter, in	5.5
Hub Diameter, in	0.825
Hub Length (min)	0.820
Number of Blades	3
Expanded Area Ratio	0.306
Blade Pitch/D @ .7R	0.718
Blade Max. Thickness/D @ .7R	0.0103
Blade Rake Angle, deg	0.
Blade Tip Skew Angle, deg	0.
Propeller RPM	1525
Vehicle Speed, kn	4.5
Speed of Advance, 1-w	0.944
Thrust, lbs	3.60
Torque, in-lbs	2.53
Developed Power, watts	45.7
QPC (efficiency)	0.811

Note that this design was predicted to result in high vessel speed, at high propulsive efficiency, with acceptable torque transmission to the vehicle, and with more than ample power margin.

Fig. 6. Final Design of REMUS Propeller



V. SYSTEM PERFORMANCE

A. System Changes.

In the late summer and fall of 1999, the proposed modifications of the vehicle and propulsion system were implemented and a casting master of the final propeller design was fabricated. Various replication techniques of the master were tried, including silicone rubber molds with castings made of high strength polyurethane, both unfilled and fiber-filled. Neither of the polyurethane techniques had the strength required for high RPMs (and power). The most durable technique has been a cast aluminum (A356) investment process for replication of the machined master.

B. Modified Design vs Previous Design

System tests of the vehicle are very encouraging but are not complete to clearly indicate where all the changes in performance have originated. However, calculated and estimated component contributions are close to the observed vehicle performance. We hope to have the opportunity to measure the vehicle drag in the tow tank, place the propulsion system on a dynamometer, and measure the propeller performance on a load stand sometime in the near future in order to define exactly where the performance gains originated.

The new design vehicle consumes 15 watts of propulsion power at 3 knots while the previous design consumed about 65 watts at 3.2 knots. The new design vehicle has a top speed of 5.6 knots drawing 110 watts of propulsion power, while the previous design had a top speed of 3.3 knots drawing 80 watts of power. See Fig 7.

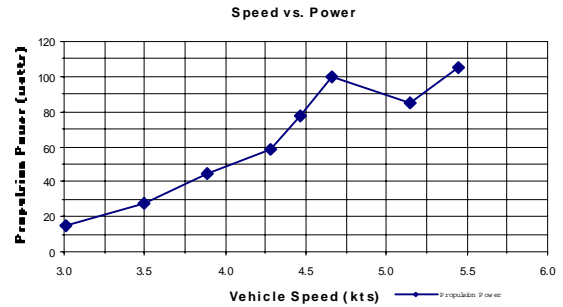


Fig.7 Speed vs Power for New Design REMUS

The performance improvements combined with a battery change from a 300 watt-hour lead-acid pack to a 1000 watt-hour lithium-ion pack bring the maximum endurance of this design up to 20+ hours at 1.5 m/s. This design has proved to be a flexible and robust platform for the addition of various sensors in addition to the sidescan sonar vehicle [9].

ACKNOWLEDGMENT

The authors would like to thank the faculty of the University of Rhode Island Ocean Engineering Department for the use and support of their tow tank facility. They would like to thank Sighard Hoerner for publishing such a durable text.

REFERENCES

- [1] C. von Alt and J.F. Grassle, "LEO-15: An Unmanned Long Term Environmental Observatory", *Proceedings Oceans 1992*, Newport, RI, 1992
- [2] C. von Alt, B. Allen, T. Austin, and R. Stokey, "Remote Environmental Monitoring Units", *Proceedings AUV 1994*, Cambridge, MA, 1994
- [3] R. Stokey and T. Austin, "Sequential Long Baseline Navigation for REMUS, an Autonomous Underwater Vehicle", *Proceedings Information Systems for Navy Divers and AUVs Operating in Very Shallow Water and Surf Zone Regions*, pp.212-219, April 1999
- [4] B. Allen, R. Stokey, T. Austin, N. Forrester, R. Goldsborough, M. Purcell, and C. von Alt, "REMUS: A Small, Low Cost AUV; System Description, Field Trials and Performance Results", *Proceedings Oceans 1997*, Halifax, Canada, 1997
- [5] M.R. Bottaccini, "The Stability Coefficients of Standard Torpedoes", NAVORD Report 3346, U.S. Naval Ordnance Test Station, China Lake, CA, 1954
- [6] Sighard F. Hoerner, *Fluid Dynamic Drag*, Published by author, 1965
- [7] D.F. Myring,, "A Theoretical Study of Body Drag in Subcritical Axisymmetric Flow", *Aeronautical Quarterly*, vol.27, pt.3, pp.186-94, August 1976
- [8] H.W.Lerbs, "Moderately Loaded Propellers with a Finite Number of Blades and an Arbitrary Distribution of Circulation", *SNAME Transactions*, 1952.
- [9] M. Purcell, C. von Alt, B. Allen, T. Austin, N. Forrester, R. Goldsborough and R. Stokey, "New Capabilities of the REMUS Autonomous Underwater Vehicle", *Proceedings Oceans 2000*, Providence, RI, September 2000